New measurement of Σ decay properties and a test of the $|\Delta I|=1/2$ rule

J. Marraffino, S. Reucroft, C. E. Roos, J. Waters, and M. Webster
Department of Physics and Astronomy, Vanderbilt University, Nashville, Tennessee 37235

A. Manz, R. Settles, and G. Wolf
Max-Planck-Institut für Physik und Astrophysik, Föhringer Ring 6, D-8000 München 40, West Germany
(Received 26 December 1979)

We report on new measurements of the Σ^+ and Σ^- lifetimes, the Σ^+ nonleptonic-decay branching ratio, and the ratio of the Σ^+ decay asymmetry parameters α_+/α_0. The final results obtained are $\tau^+ = (0.798 \pm 0.005) \times 10^{-10}$ sec, $\tau^- = (1.480 \pm 0.014) \times 10^{-10}$ sec, $R = \Gamma(\Sigma^+ \to p\pi^0)/\Gamma(\Sigma^+ \to \text{all}) = 0.5172 \pm 0.0036$, and $\alpha_+/\alpha_0 = -0.073 \pm 0.021$. These results together with the world average for α_0 are used to perform a test of the $|\Delta I| = 1/2$ rule.

I. INTRODUCTION

In this paper, we report new measurements of several properties of Σ^+ nonleptonic decays along with a new test of the $|\Delta I| = \frac{1}{2}$ rule. On the basis of a sample of approximately 120 000 Σ^+ decays, we have determined values for the lifetimes, the Σ^+ nonleptonic-decay branching ratio $R = \Gamma(\Sigma^+ \to p\pi)/\Gamma(\Sigma^+ \to \text{all})$, and the ratio of the asymmetry parameters for decays, α_+/α_0, with statistical errors that are of the order of those on the present world averages. These data were obtained as part of a high-statistics experiment to measure μ_{Σ^+}, the magnetic moment of the Σ^+ hyperon.[1] In that connection, verifying that reasonable values for all of these parameters were obtained with the μ_{Σ^+} sample constituted a crucial test of the quality of the data used in the measurement of μ_{Σ^+}. Moreover, new and precise measurements of these fundamental properties of the Σ hyperons are important in their own right.

In Sec. II, we briefly review those details of the experimental apparatus and of our analysis of the data which are common to all three measurements. The determinations of lifetimes, branching ratios, and asymmetry parameters are discussed in detail separately in Secs. III, IV, and V, respectively. We then combine all of our measurements in Sec. VI to perform a test of the $|\Delta I| = \frac{1}{2}$ rule and present a discussion of our results.

II. EXPERIMENTAL APPARATUS AND METHODS

The hyperon bubble chamber (HYBUC) was built by the Max-Planck-Institut für Physik and Astrophysik and by Vanderbilt University, specifically for the measurement of the Σ^+ magnetic moment.[1] HYBUC is a cylindrical liquid-hydrogen bubble chamber with a useful volume 32 cm long and 11 cm in diameter surrounded by an 11-T superconducting solenoid. Many of the technical features of HYBUC have been discussed elsehwhere[1-5] and hence need not be repeated here except to emphasize once more two important design criteria. These are the following:

(i) The detection efficiency should be as nearly isotropic as possible in order to minimize instrumental biases.

(ii) The measuring accuracies on angles and momenta should be as high as possible in order to obtain the required precision.

Since it was necessary to obtain a large sample of polarized Σ hyperons, we needed to find a production reaction in which the cross section and the polarization were simultaneously large. A study of the then existing phase-shift analyses[6] led to the choice of

$$K^- p \to \Sigma^{\pm} \pi^{\mp} \tag{1}$$

at beam momenta in the interval 420–500 MeV/c. The beam was derived from an internal target in the CERN proton synchrotron and was a two-stage, electrostatically separated beam 16 m long. The momentum bite of this beam was ±1% with a final image 4 mm in diameter positioned approximately 50 cm upstream of the fiducial volume of the bubble chamber. For 10^{11} protons at 20 GeV/c on our target, this beam delivered an average of 8 K^- per picture with a muon contamination of less that 10%.

A total of 2.4×10^6 pictures were taken in 2500 hours of running. Approximately 20% of this film, mostly from the very early running, was discarded due to poor beam or chamber operation. The remaining film represents a total exposure of $1.5 \times 10^{-} K^-$. These data were taken at nominal beam momenta of 440, 460, 480, and 500 MeV/c distributed roughly in the ratio 1 : 6 : 4 : 3.

The good films were doubly scanned, and events with the two-prong charged-V topology were mea-

sured on manual machines both at the Max-Planck-Institut and at Vanderbilt University. The data were processed by the HYDRA system[7] geometry/kinematics programs. Each event, together with printed output from the computer was reexamined at the scanning table to check for consistency between the kinematic fits and track ionization. In the case of Σ^+ production, the competing hypotheses are mainly

$$K^-p \to \Sigma^+\pi^- \text{ and } K^-p \to \Sigma^+\pi^- . \qquad (2)$$
$$\searrow p\pi^0 \qquad\qquad \searrow n\pi^+$$

In the case of Σ^- production, the competing hypotheses are mainly

$$K^-p \to \Sigma^-\pi^+ \text{ and } K^-p \to K^-p . \qquad (3)$$
$$\searrow n\pi^- \qquad\qquad \searrow \mu^-\nu \text{ or } \pi^-\pi^0$$

The track ionization could readily distinguish between these hypotheses.

All events which failed to give a two-vertex fit which agreed with observed track ionization were remeasured, and those which failed again were measured yet again. After this procedure, the residual failure rate was 5%. Upon subsequent study of these "hard-core" failures, we were able to ascertain that no more than 10% of them were indeed two-body Σ events. Our overall scanning efficiency was calculated to be at least 99%. This does not, however, include an estimated systematic loss of 7% of the $\Sigma^+ \to p\pi^0$ events where the laboratory angle between the Σ^+ and the decay proton was unobservably small, or either the Σ^+ or p track was unobservably short. Small-angle decay losses, while observed, were significantly less severe in the $\Sigma^+ \to n\pi^+$ and $\Sigma^- \to n\pi^-$ channels. Losses due to very short hyperon tracks were also noted and had approximately the same severity in all channels. These losses and their effect on our measurements are dealt with in detail in the following sections.

To enhance the overall quality of the data to be used for physics analysis, the following set of general cuts was imposed:

(i) The production vertex was required to lie at least 2 cm downstream of the entrance window and at least 6 cm upstream of the exit window of the bubble chamber.

(ii) The missing mass at the production vertex, calculated using the results of the geometry program and excluding the hyperon track, was required to lie in the interval from 1.1 to 1.3 GeV/c^2.

(iii) The reconstructed beam momentum was required to lie in the interval from 0.43 to 0.51 GeV/c after accounting for energy loss in the chamber medium.

(iv) All hyperon tracks were required to have a laboratory length of at least 0.3 cm.

III. MEASUREMENT OF THE Σ^+ AND Σ^- LIFETIMES

In this section, we discuss our determination of the lifetimes $\tau^\pm$ of the $\Sigma^\pm$ hyperons and describe the procedures used. As has already been observed, all three Σ decay channels suffered losses due to very short Σ tracks. To further purify our data sample for the lifetime measurements, in addition to the general cuts outlined above, we have also rejected all events for which the hyperon momentum was less than 0.2 GeV/c. Furthermore, the minimum projected track-length cut was made more stringent as described below. These two additional cuts removed all of those events which were prone to scanning biases. For a minimum projected length cut of 3 mm, we are left with 37 000 Σ^+ and 32 000 Σ^- candidates.

We used the maximum-likelihood method for our fit to the hyperon lifetimes. This required the construction of a properly normalized probability density function for the hyperon decay. In terms of the mean decay length l_0 and the laboratory track length l in the interval between l_L (lower) and l_U (upper), that probability density function is

$$P(l;l_0) = \frac{e^{-l/l_0}}{l_0(e^{-l_L/l_0} - e^{-l_U/l_0})} . \qquad (4)$$

It is more convenient, however, to work with the proper time t in order to obtain

$$P(t;\tau) = \frac{e^{-t/\tau}}{\tau(e^{-t_L/\tau} - e^{-t_U/\tau})} , \qquad (5)$$

where t is required to lie in the interval between lower and upper limits, t_L and t_U, and τ is the lifetime. The numbers t_L and t_U are defined, event by event, as the minimum and maximum proper times observable within the limits imposed on the minimum projected length l_L and the maximum path length l_U. This maximum path length is, in turn, defined either by the length of the hyperon trajectory at which the particle would have left the fiducial volume, or by the length of the trajectory at which the particle would have stopped in the bubble chamber, or by a fixed upper limit, whichever is smallest. The energy loss in the liquid hydrogen has been taken into account in the calculation of all proper times.

The above development of $P(l;l_0)$ assumes that the track lengths l and, correspondingly, the proper times t are known to infinite precision. This is, however, not the case. In the case of

the Σ^+ hyperon, the mean track length is 1.0 cm with a mean error of 0.03 cm. For the Σ^- events, the mean track length is 1.6 cm, again with a mean error of 0.03 cm. Our attempt to account for the error in track length is described in the following paragraphs.

We assume that the track-length error, Δl, has a Gaussian distribution with zero mean and variance σ. Thus, the probability for a length error of Δl is

$$P(\Delta l) = \frac{1}{\sqrt{2\pi}\sigma} e^{-(\Delta l)^2/2\sigma^2} . \tag{6}$$

Then the numerator of the probability density in Eq. (4) becomes

$$\frac{1}{2l_0} e^{\sigma^2/2l_0^2} \operatorname{erfc}(m) e^{-l/l_0} ,$$

where

$$m = \frac{1}{\sqrt{2}\sigma}\left(\frac{\sigma^2}{l_0} - l\right),$$

and $\operatorname{erfc}(m)$ is the complementary error function defined by

$$\operatorname{erfc}(m) = \frac{2}{\sqrt{\pi}} \int_m^\infty e^{-z^2} dZ . \tag{7}$$

The error distribution in Eq. (6) is imposed on the laboratory track length, which is the actually measured variable. However, to determine the lifetime τ, we again deal with proper times. If we again write $l = \beta\gamma ct = \eta x$, where $\eta = \beta\gamma$ and $x = ct$, and normalize between x_L and x_U, we find

$$P(x;x_0) = \frac{\operatorname{erfc}(m) e^{-x/x_0}}{x_0\{[\operatorname{erfc}(m_L)e^{-x_L/x_0} - \operatorname{erfc}(m_U)e^{-x_U/x_0}] + \exp(-\sigma^2/2\eta^2x_0^2)[\operatorname{erfc}(z_L) - \operatorname{erfc}(z_U)]\}} , \tag{8}$$

where

$$m_L = \frac{1}{\sqrt{2}\sigma}\left(\frac{\sigma^2}{\eta x_0} - \eta x_L\right), \quad m_U = \frac{1}{\sqrt{2}\sigma}\left(\frac{\sigma^2}{\eta x_0} - \eta x_U\right),$$

$$z_L = \frac{1}{\sqrt{2}\sigma}\eta x_L, \quad z_U = \frac{1}{\sqrt{2}\sigma}\eta x_U, \quad x_0 = c\tau ,$$

and σ is obtained event by event from the geometry program. We point out that, as $\sigma \to 0$, Eq. (8) reduces to Eq. (5) as expected. The likelihood function is then defined as

$$\mathcal{L}(x;x_0) = \prod_{i=1}^{N} P_i(x;x_0) ,$$

the product being taken over the N observed decays. The best value of $x = c\tau$ is that value which maximizes $\mathcal{L}(x;x_0)$ or, equivalently, $\ln\mathcal{L}(x;x_0)$. We have performed this fit for the two Σ^+ decay modes separately for a set of values of x_L and x_U and, after noting no significant differences between the results, repeated the calculation with all Σ^+ decays combined. We have determined the error in $c\tau$ by finding the value of x for which $\ln\mathcal{L}$ decreases by 0.5 from its maximum. For a short cutoff corresponding to 0.4 cm in projected length and a long cutoff corresponding to 15 cm, we obtain $c\tau^+ = 2.391 \pm 0.015$ cm from 30 024 Σ^+ events. This gives $\tau^+ = (0.798 \pm 0.005) \times 10^{-10}$ sec. Similarly, from 15 544 Σ^- decays, with a short cutoff corresponding to 0.6 cm in projected length and a long cutoff corresponding to 20 cm, we obtain $c\tau^- = 4.438 \pm 0.043$ cm, or $\tau^- = (1.480 \pm 0.014) \times 10^{-10}$ sec.

The short and long cutoff values were chosen according to the following method. For a given long cutoff, the short cutoff was varied from 0.1 to 0.8 cm. Because of the short-track losses, the fitted lifetime is rather large for the shortest cutoff value, but drops and stabilizes as the cutoff value is increased. This is shown in Fig. 1. We have quoted the lifetime corresponding to the shortest

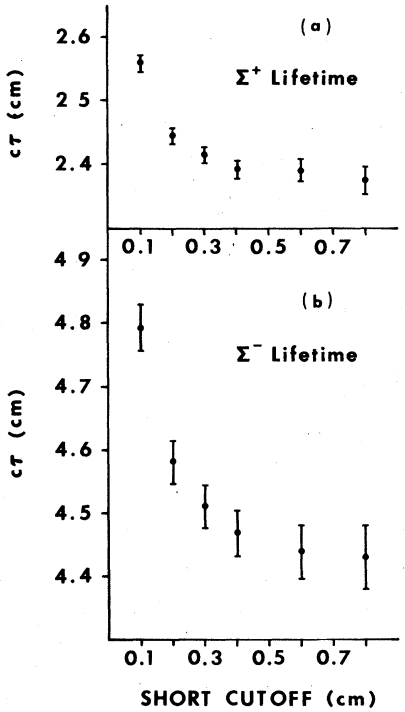

FIG. 1. Variation of $c\tau$ with short cutoff for (a) Σ^+ decay with a 15-cm long cutoff, and (b) Σ^- decay with a 20-cm long cutoff.

cutoff value in the stable region. In the case of the Σ^+ data, the lifetime was observed to be quite insensitive to the long cutoff. On the other hand, the fit to the Σ^- data was found to be more sensitive to the long cutoff value, possibly due to a very small reduction in scanning efficiency for the events with very long hyperon tracks. Losses due to interactions in flight were negligible. The final value of 20 cm was again chosen on the basis of the stability of the fitted lifetime. To test that the data-selection criteria, as well as our choice of cutoff values, were indeed appropriate, we have plotted the hyperon lifetime as a function of the hyperon momentum in Fig. 2. Since neither τ^+ nor τ^- shows any significant dependence on p_Σ, we conclude that no length-dependent biases remain. We also note in passing that, for the short cutoff values finally chosen, we observed no differences between the lifetimes obtained by fitting Eq. (8) and those obtained by fitting Eq. (5).

IV. MEASUREMENT OF THE Σ^+ BRANCHING RATIO

In distinction to the measurement of $\tau^\pm$, where uniform detection efficiency independent of hyperon track length is necessary, the determination of the Σ^+ branching ratio requires identical detection efficiencies for the decay modes in question. As already mentioned in Sec. II, our detection efficiency for $\Sigma^+ \to p\pi^0$ is not identical to that for $\Sigma^+ \to n\pi^+$ because for $\Sigma^+ \to p\pi^0$ there are more decays for which the laboratory angle between the Σ^+ and decay proton is too small to be seen. This can be made more quantitative in the following way. We define $\hat{n}$ as a unit vector normal to the production plane such that $\hat{n} = \hat{K} \times \hat{\pi} / |\hat{K} \times \hat{\pi}|$, where $\hat{K}$ is a unit vector in the beam direction and $\hat{\pi}$ is a unit vector in the direction of the produced pion. Further, we define $\hat{p}$ as a unit vector in the direction of the decay nucleon in the hyperon rest frame. Then, the angular distribution for the Σ decay is given by

$$\frac{dN}{d\cos\xi} = \tfrac{1}{2}N[1 + \alpha P \cos\xi], \tag{9}$$

where $\cos\xi = \hat{n} \cdot \hat{p}$, α is the asymmetry parameter for the decay mode under investigation, and P is the magnitude of the Σ polarization. Figure 3 shows these distributions for our data, and losses can be clearly seen in the region of $\cos\xi$ around zero. It is a consequence of the HYBUC geometry that events for which (a) the laboratory decay angle is very small, (b) the charged decay particle is very short, or (c) the charged decay particle is parallel to the field and therefore has a poorly determined momentum, all lie in a $\cos\xi$ interval around zero. By making symmetric cuts about $\cos\xi = 0.0$, we eliminate all scanning losses, and

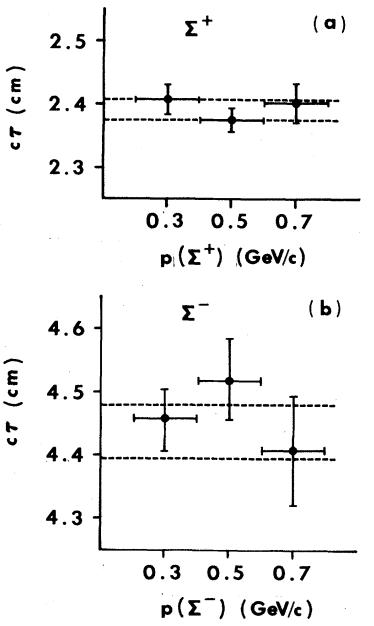

FIG. 2. Variation of $c\tau$ with Σ momentum for (a) Σ^+ decay, and (b) Σ^- decay. The dashed horizontal lines indicate ± 1 standard deviation from our fitted values as discussed in the text.

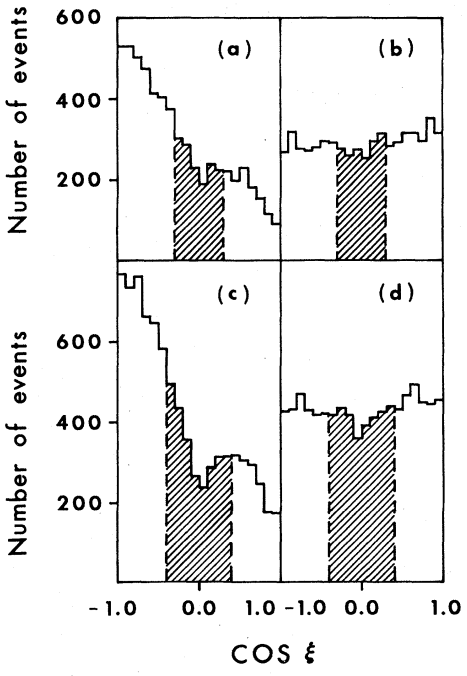

FIG. 3. Distributions of $\cos\xi$ as defined in the text: (a) Vanderbilt $\Sigma^+ \to p\pi^0$ data, (b) Vanderbilt $\Sigma^+ \to n\pi^+$ data, (c) MPI $\Sigma^+ \to p\pi^0$ data, and (d) MPI $\Sigma^+ \to n\pi^+$ data. The shaded regions have been excluded for the branching-ratio determination.

most of the events producing zero-constraint (0C) kinematics fits due to poorly determined charged-decay-particle momenta. If we define the production angle θ^* as $\cos\theta^* = \hat{K}\cdot\hat{\pi}$ (now in the production center-of-mass frame) and demand that $\cos\theta^*$ lie in the interval $-0.5 < \cos\theta^* < 0.75$, we eliminate the remainder of the 0C ambiguous fits.

Because the scanning procedures at the two laboratories were slightly different, the branching ratio was calculated for the two data samples separately and the results were later combined. In the Vanderbilt sample, with all of the general cuts described in Sec. II, the $\cos\theta^*$ cut defined above, and requiring that $\cos\xi > 0.3$, we find 4416 proton and 4156 π^+ decays. There is, in addition, a correction for missed Dalitz pair decays, i.e.,

$$\Sigma^+ \to p\pi^0, \quad \pi^0 \to e^+e^-\gamma$$

to consider. This correction is small (at most 1%) and we do not know whether other experimenters have accounted for it. We have computed this correction as a multiplicative factor on the number of $\Sigma^+ \to p\pi^0$ decays. That factor varies from 1.0116 to 1.0 as the efficiency for detecting Dalitz pairs varies from 0% to 100%. In the case of the Vanderbilt data, the correction factor is 1.0093 ± 0.0010 which then leads to

$$R = \frac{\Gamma(\Sigma^+ \to p\pi^0)}{\Gamma(\Sigma^+ \to \text{all})} = 0.5175 \pm 0.0055 .$$

All of the above cuts were applied to the Max-Planck-Institut (MPI) data as well except that the $\cos\xi$ cut was chosen as $|\cos\xi| > 0.4$. Then we find 5657 proton decays and 5318 π^+ decays. The MPI Dalitz-pair correction factor was found to be 1.0062 ± 0.0014, yielding a branching ratio of $R = 0.5170 \pm 0.0049$. Combining the two samples finally yields $R = 0.5172 \pm 0.0036$.

V. MEASUREMENT OF α_+/α_0

We have already published[8] a preliminary value for the ratio α_+/α_0 based on the Σ^+ decay angular distribution given earlier in Eq. (9). The angle ξ used in that expression should be the angle between the Σ spin and the decay baryon momentum at decay. We point out that in our previous paper our use of Eq. (9) was, at least in principle, slightly incorrect in that we had taken the polarization direction as the normal to the production plane. That vector does not represent the polarization of the Σ at the point of decay because of the precession of the Σ spin in the magnetic field.

This effect, while small, can now be dealt with properly since we have now measured the Σ^+ magnetic moment.[1] In a coordinate system in which the Σ is at rest and which turns with the Σ in the magnetic field, the polarization $\vec{P}$ precesses according to[9]

$$\frac{d\vec{P}}{d\tau} = \mu_a \frac{e}{mc}(\vec{P}\times\vec{B}'), \tag{10}$$

where τ is the proper time, m the Σ mass, μ_a the anomolous moment of the Σ, and $\vec{B}'$ the magnetic induction in the Σ rest frame. Following the complete derivation given in Ref. 1, we then obtain the angular distribution

$$\frac{1}{N}\frac{dN}{d\Omega} = \frac{1}{2\pi}\left[1 + \frac{\pi}{4}\alpha P_\perp \cos(\phi - \phi_0)\right], \tag{11}$$

where ϕ is the angle of the projection of the decay baryon momentum into the plane normal to $\vec{B}'$, and $P_\perp$ is the component of the hyperon polarization transverse to $\vec{B}'$. The angle ϕ is measured from $\vec{P}_0$, the hyperon polarization direction at decay for $\mu_a = 0$. For a Σ decaying after a proper time τ, ϕ_0 is defined by $\mu_a e c\tau B'/mc^2$, where m is the Σ mass and $B' = B'$. If we interpret this as the expected probability density for ϕ, we can again form the likelihood function

$$\mathcal{L}(\phi; \alpha P_\perp) = \prod_{i=1}^{N}\left[1 + \frac{\pi}{4}\alpha P_\perp \cos(\phi_i - \phi_0)\right],$$

where ϕ_0 is given above and $\mu_{\Sigma^+} = 1.916$ from our previous measurement. Without a measurement of the polarization of the decay baryon, α and P cannot be determined separately. Thus, we maximize the function $\mathcal{L}(\phi; \alpha P)$ with respect to $\alpha_0 P_\perp$ to obtain $\alpha_0 P_\perp$ from the $\Sigma^+ \to p\pi^0$ mode, and $\alpha_+ P_\perp$ from the $\Sigma^+ \to n\pi^+$ mode.

The distributions for our data are shown in Fig. 4 and, once again, the losses noted earlier are evident. No cuts beyond those described in Sec. II have been imposed on the data shown. However, two additional cuts are necessary in what follows. As in Sec. IV, we require $-0.5 < \cos\theta^* < 0.75$, where $\cos\theta^*$ has been defined above. This cut eliminates many of the 0C ambiguous events and, at the same time, has little effect on the statistical significance of the fit result, since only events with relatively-low-polarization hyperons are excluded. We eliminate the remainder of the biases by making additional cuts directly in the ϕ distribution by excluding all events for which ϕ is within ±20° of −90° or +90° (shaded area in Fig. 4). Except for the effect of the precession of the Σ^+ polarization in the magnetic field, this cut in ϕ is completely equivalent to a cut in $\cos\xi$, as was imposed in the determination of R (see Sec. IV). It is much more convenient here to cut in ϕ because then the normalization of $\mathcal{L}(\phi; \alpha P)$ can be calculated analytically. Excluding all events with $\phi_1 < \phi < \phi_2$ and $\phi_3 < \phi < \phi_4$, we rewrite Eq. (11) as

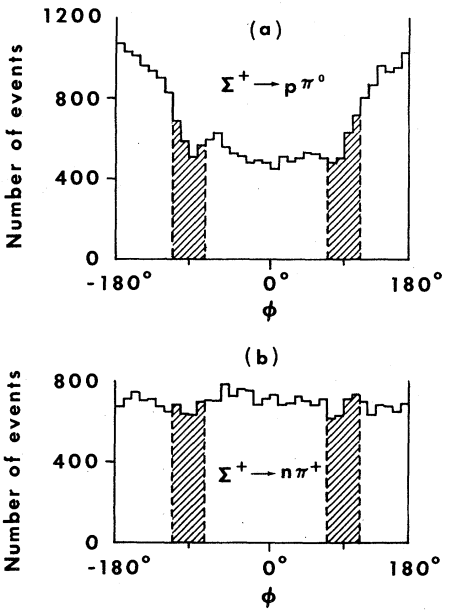

FIG. 4. Distribution of Σ precession angle for (a) $\Sigma^+ \to p\pi$ events, and (b) $\Sigma^+ \to n\pi^+$ events. The shaded regions have been excluded for the determination of $\alpha A/\alpha_0$.

$$\frac{1}{N}\frac{dN}{d\Omega} = \frac{1}{K}\left[1 + \frac{\pi}{4}\alpha P_\perp \cos(\phi - \phi_0)\right], \tag{12}$$

where the correct normalization factor is given by

$$K = 2\pi + \phi_1 - \phi_2 + \phi_3 - \phi_4 + \frac{\pi}{4}\alpha P_\perp[\sin\phi_0(\cos\phi_2 - \cos\phi_1 + \cos\phi_4 - \cos\phi_3) - \cos\phi_0(\sin\phi_2 - \sin\phi_1 + \sin\phi_4 - \sin\phi_3)].$$

These cuts reduce the data sample to 11 841 $\Sigma^+ \to p\pi^0$ events and 11 376 $\Sigma^+ \to n\pi^+$ events.

Since P is a function of $\cos\theta^*$, we have performed the fit to $\alpha_+ P_\perp$ and $\alpha_0 P_\perp$ in ten $\cos\theta^*$ bins separately, determined the ratio α_+/α_0 for each bin, and then averaged these values together. Table I gives a summary of these results from which we finally obtain $\alpha_+/\alpha_0 = -0.073 \pm 0.021$. The difference between this value and our previously published value of -0.104 ± 0.028 is too large to be ascribed to the fact that we have now properly considered the effect of μ_{Σ^+}. That preliminary value was based on a subsample of our present data. Since then, the remainder of the data has been added, additional track-ionization decisions have been made, and the optical and magnetic field constants have been improved, as well as the geometry/kinematics programs. Moreover, the error on our earlier measurement of α_+/α_0 was purely statistical and did not include the systematic effects treated here.

TABLE I. Fit to α_+/α_0 as a function of $\cos\theta^*$.

$\cos\theta^*$	$\alpha_0 P$	$\alpha_+ P$	$\alpha_+ P/\alpha_0 P$
−0.9			
−0.7			
−0.5	-0.2736 ± 0.0458	0.0574 ± 0.0508	-0.210 ± 0.189
−0.3	-0.4456 ± 0.0343	0.0288 ± 0.0370	-0.065 ± 0.083
−0.1	-0.5441 ± 0.0344	0.0470 ± 0.0374	-0.086 ± 0.069
0.1	-0.7081 ± 0.0256	0.0894 ± 0.0387	-0.126 ± 0.055
0.3	-0.8403 ± 0.0249	0.0585 ± 0.0371	-0.070 ± 0.044
0.5	-0.9209 ± 0.0252	-0.0014 ± 0.0383	0.002 ± 0.042
0.7	-0.9262 ± 0.0326	0.1196 ± 0.0461	-0.129 ± 0.050
0.9			
		Average: -0.073 ± 0.021	

We can, in addition, obtain some information on α_+ and α_0 separately by referring to any of several phase-shift analyses in the literature (see, for instance, Refs. 10 and 11). There are, however, two details that must be discussed briefly first.

The geometry of HYBUC is such that the beam is parallel to the magnetic field. As a consequence, the Σ polarization at production is transverse to $\vec{B}$. Then $\vec{P}$ can only develop a component along $\vec{B}'$ because of the precession of the polarization through the anomalous magnetic moment, or because of the small rotation implicit in the Lorentz transformation of B to the Σ rest frame. Both of these effects are quite small and average to zero due to the axial symmetry of our apparatus and because half the data have B parallel to the beam and half have B antiparallel. We shall hence ignore them, and replace $P_\perp$ by P. In addition, Kp phase-shift analyses in our energy region are generally performed assuming that $\alpha_0 = -1.0$. This has the effect of slightly underestimating the Σ polarization but gives a correct parametrization of the dependence on $\cos\theta^*$. This is sufficient for our purposes here.

If we use the results of Gopal *et al.*[11] to represent $P(\cos\theta^*)$ and maximize $\mathcal{L}(\phi; \alpha P)$ with respect to α alone, we obtain $\alpha_0 = -1.0119 \pm 0.0158$ and $\alpha_+ = 0.0706 \pm 0.0206$. The fact that we find $\alpha_0 = -1.0$ within errors is a direct consequence of the assumption that $\alpha_0 = -1.0$ as discussed above. If we further scale the result by the ratio of the world-average value for α_0 as given by the Particle Data Group[12] to the assumed value -1, we find $\alpha_+ = 0.0690 \pm 0.0201$ in excellent agreement with the Particle Data Group.

VI. TEST OF THE $|\Delta I| = \frac{1}{2}$ RULE AND DISCUSSION

We can now use all the above values of lifetimes, branching ratios, and asymmetry parameters, together with our previously published value of α_-,[8]

namely $\alpha_- = -0.062 \pm 0.024$, to extract the s-wave and p-wave amplitudes in Σ decay. Following a suggestion of Jackson as given by Overseth,[13] we use dimensionless amplitudes A and B related to s and p by the relation

$$\frac{p}{s} = \left[\frac{(M-m)^2-\mu^2}{(M+m)^2-\mu^2}\right]^{1/2} \frac{B}{A} = C_1 \frac{B}{A}\,, \tag{13}$$

where M, m, and μ are the Σ, decay-baryon, and decay-pion masses, respectively, and C_1 is the square root of the expression in square brackets in Eq. (13). The partial decay rate is given in terms of A and B by

$$\Gamma = \frac{G^2 \mu_c^{\,4}}{8\pi}\, q \left\{ \left[\frac{(M+m)^2-\mu^2}{M^2}\right] |A|^2 + \left[\frac{(M-m)^2-\mu^2}{M^2}\right] |B|^2 \right\}, \tag{14}$$

where $G^2 \mu_c^{\,4}/8\pi = 1.9488 \times 10^{-15}$, and q is the pion momentum in the Σ rest frame. Under the assumptions of time-reversal invariance and no final-state interactions, A and B are relatively real and we may write

$$\alpha = \frac{2C_1 B/A}{1 + C_1^{\,2}(B/A)^2}\,. \tag{15}$$

Taking Eqs. (14) and (15) together, we then obtain

$$\begin{aligned} B^2 &= \Gamma (C_2 \{[1 \pm (1-\alpha^2)^{1/2}]^2/\alpha^2 + 1\})^{-1}\,, \\ A &= C_1 B [1 \pm (1-\alpha^2)^{1/2}]/\alpha\,, \end{aligned} \tag{16}$$

where

$$C_2 = G^2 \mu_c^{\,4} q [(M-m)^2 - \mu^2]/8\pi M^2$$

and the signs are chosen such as to satisfy approximately the $|\Delta I| = \frac{1}{2}$ rule.

This rule requires that the Σ decay amplitudes A and B separately satisfy

$$\sqrt{2}\,\Sigma_0 + \Sigma_+ - \Sigma_- = 0\,, \tag{17}$$

where the subscripts refer to the charge of the decay pion. Plotted in the A-B plane, these vectors would form a closed triangle. Including $|\Delta I| > \frac{1}{2}$ transitions, we have more generally

$$\sqrt{2}\,\Sigma_0 + \Sigma_+ - \Sigma_- = 3\left(\tfrac{2}{5}\right)^{1/2} \Sigma_{3/2} + \left(\tfrac{2}{15}\right)^{1/2} \Sigma_{5/2}\,,$$

where $\Sigma_{3/2}$ and $\Sigma_{5/2}$ are the $|\Delta I| = \frac{3}{2}$ and $|\Delta I| = \frac{5}{2}$ amplitudes, respectively.

We calculate two sets of A and B amplitudes: The first uses the results of this experiment for all input quantities except for α_0 which we take from the Particle Data Group; the second uses averages of our results with the former world averages. Our previous measurement of α_+ has been omitted from the world average since the value determined here replaces it.

Previous determinations of α_+ and α_- have used various phase-shift analyses to calculate the polarization P. We have used one set of phase shifts[11] for both α_+ and α_-. It must be emphasized again that the phase-shift analyses assume some value for α_0 (in our case -1.0). This introduces correlations between the asymmetry parameters and hence between the amplitudes as calculated from Eq. (16). The A_+ and B_- amplitudes are approximately linear in α while A_- and B_+ are to first order independent of α.

Table II presents the calculated values of the A and B amplitudes from the two sets of input values used. For our data alone, these amplitudes are plotted in Fig. 5. For readers who prefer to see s and p amplitudes plotted, we point out that $C_1 \approx \frac{1}{10}$, and our A and B axis scales are in the ratio 1 : 10.

We have calculated how well Eq. (17) is satisfied for the A and B amplitudes below:

$$\begin{aligned} \sqrt{2}\,A_0 + A_+ - A_- &= 0.22 \pm 0.08 \quad \text{(this experiment)} \\ &= 0.24 \pm 0.08 \quad \text{(world average)}\,, \\ \sqrt{2}\,B_0 + B_+ - B_- &= 2.66 \pm 1.00 \quad \text{(this experiment)} \\ &= 2.72 \pm 1.00 \quad \text{(world average)}\,. \end{aligned}$$

Before commenting on these results, we must first make a few observations about errors. In the calculation of the above errors, the correlations of α_+ and α_- with α_0 have been taken into account such that

$$\alpha_+ = -\alpha_+^m \alpha_0\,, \quad \alpha_- = -\alpha_-^m \alpha_0\,,$$

where $\alpha_\pm^m$ are the values obtained using polarization fits from phase shifts assuming $\alpha_0 = -1.0$. The above errors are, however, largely meaningless beyond 1 standard deviation. We note that α_0 is within 1.5 standard deviations of the physical limit. If we write B from Eq. (16) as $B = \pm(\Gamma/C_2)^{1/2}/f(\alpha)$, and plot $f(\alpha)$ near $\alpha = -1.0$ (see Fig. 6), we see that $f(\alpha)$ is steep and drops sharply as $\alpha \to -1.0$. In fact, the first derivative of $f(\alpha)$ becomes singular at $\alpha = -1.0$. Calling the

TABLE II. A and B amplitudes for Σ decay.

Decay mode	A	B
	This experiment	
$\Sigma^+ \to p\pi^0$	1.48 ± 0.05	-12.03 ± 0.57
$\Sigma^+ \to n\pi^+$	0.064 ± 0.019	19.07 ± 0.09
$\Sigma^- \to n\pi^-$	1.933 ± 0.009	-0.59 ± 0.22
	World average	
$\Sigma^+ \to p\pi^0$	1.48 ± 0.05	-12.01 ± 0.57
$\Sigma^+ \to n\pi^+$	0.065 ± 0.013	19.05 ± 0.08
$\Sigma^- \to n\pi^-$	1.921 ± 0.007	-0.65 ± 0.08

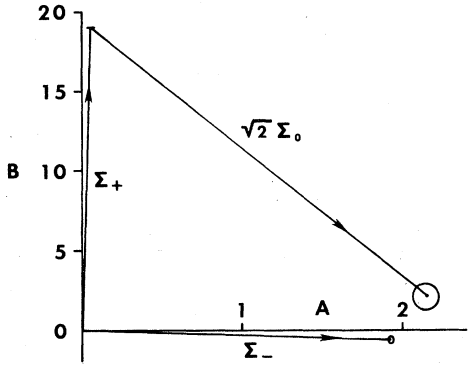

FIG. 5. Dimensionless amplitudes A and B as determined from this experiment alone. The nonclosure of the "Σ^- triangle" shows the extent of the observed violation of the $|\Delta I| = \frac{1}{2}$ rule.

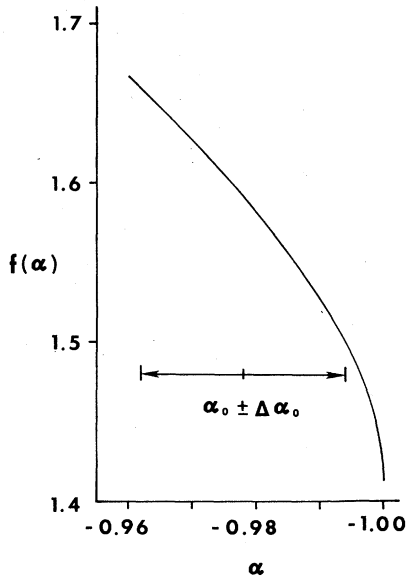

FIG. 6. Variation of $f(\alpha)$, as defined in the text, with α in the vicinity of α_0.

world-average value $\bar{\alpha}_0$, we have indicated $\bar{\alpha}_0 \pm \Delta\alpha$ in Fig. 6. We see that the error in B is not linear, and that in the vicinity of $\alpha_0 = -1.0$ the usual linear error propagation is at best only marginally valid. Thus, while our results seem to indicate a 2-to-3-standard-deviation violation of the $|\Delta I| = \frac{1}{2}$ rule, it seems to us too superficial to interpret them in that way.

The results obtained here, using data from a single experiment and one set of phase shifts, are the same as those obtained by Overseth[13] using all previous data. The uncertainties in the sums in Eq. (17) are dominated by the errors in A_0 and B_0 together with the correlations with A_+ and B_- which follow from the correlations of $\alpha_\pm$ with α_0. Furthermore, the amplitudes A_0 and B_0 are very sensitive to α_0 and not to Γ_0, viz.,

$$\frac{\partial B_0}{\partial \alpha_0} \approx 3B_0, \quad \frac{\partial B_0}{\partial \Gamma_0} = \frac{B_0}{2\Gamma_0} .$$

We can conclude then that a significant improvement in the determination of A_0 and B_0, which would lead to a much more stringest test of the $|\Delta I| = \frac{1}{2}$ rule, must await a still more precise measurement of α_0.

Because A_+ and B_- are proportional to $\alpha\sqrt{\Gamma}$, our improved resolution on Γ does not significantly reduce the errors on these two amplitudes. On the other hand, A_- and B_+ are to first order independent of α, and we have reduced the errors on these amplitudes.

ACKNOWLEDGMENTS

We are indebted to many people for their ready aid in the successful completion of this work. Although the following list is by no means exhaustive, we would certainly be remiss without expressing our thanks to E. Dahl-Jensen, I. Dahl-Jensen, N. Doble, K. Gottstein, I. Herynek, Ch. Peyrou, A. Poppleton, F. Schmeissner, T. Hansl, and W. Matt. The contributions of the technical staff at Vanderbilt University, the Max-Planck-Institut, and CERN were many and are deeply appreciated. The scanning and measuring staff at Vanderbilt and the Max-Planck-Institut are likewise gratefully acknowledged for a difficult job well done. Professor N. Schmitz of the Max-Planck-Institut must also be thanked for his long and continuing support of this work. This work was supported by the Bundesministerium für Forschung und Technologie of the Federal Republic of Germany and by the National Science Foundation of the United States of America under Grant No. 073-08392.

[1]R. Settles, A. Manz, W. Matt, T. Hansl, I. Herynek, N. Doble, G. Wolf, S. Reucroft, J. Marraffino, J. Waters, M. Webster, and C. E. Roos, Phys. Rev. D 20, 2154 (1979).

[2]D. Coffey, A. Manz, R. Settles, S. Reucroft, and C. E. Roos, Nucl. Instrum. Methods 150, 377 (1978).

[3]A. Manz, S. Reucroft, and R. Settles, Rutherford Laboratory Report No. RHEL/R271, 1971 (unpublished), p. 48.

[4]R. Settles, A. Manz, J. Marraffino, T. Hansl, S. Reu-

croft, and Ch. Peyrou, Nucl. Instrum. Methods 125, 435 (1975).
[5]A. Manz, R. Settles, G. Wolf, G. Poppleton, and B. Powell, Oxford Conference on Computer Scanning, 1974 (unpublished), p. 751.
[6]R. Armenteros, P. Ballion, C. Bricman, M. Ferro-Luzzi, D. E. Plane, N. Schmitz, E. Burkhardt, H. Filthuth, E. Kluge, H. Oberlack, R. R. Ross, R. Barloutaud, P. Granet, J. Meyer, J. P. Porte, and J. Prevost, Nucl. Phys. B14, 91 (1969).
[7]HYDRA Application Library, CERN/EP Division, 1976 (unpublished).
[8]T. Hansl, A. Manz, W. Matt, S. Reucroft, R. Settles, J. W. Waters, G. Wolf, H. Fenker, J. M. Marraffino, C. E. Roos, and M. S. Webster, Nucl. Phys. B132, 45 (1978).
[9]V. Bargmann, L. Michel, and V. L. Telegdi, Phys. Rev. Lett. 2, 435 (1959).
[10]V. Hepp, O. Braun, H. J. Grimm, H. Strobele, C. Thol, T. S. Thouw, F. Gandini, C. Kiesling, D. E. Plane, and W. Wittek, Phys. Lett. 65B, 487 (1976).
[11]G. P. Gopal, R. T. Ross, A. J. Van Horn, A. C. McPherson, E. F. Clayton, T. C. Bacon, and I. Butterworth, Nucl. Phys. B119, 362 (1976).
[12]Particle Data Group, Phys. Lett. 75B, 1 (1978).
[13]O. E. Overseth, Phys. Lett. 75B, 241 (1978).